JOURNAL OF VIROLOGY, Jan. 2006, p. 941–950 Vol. 80, No. 2
0022-538X/06/$08.00+0 doi:10.1128/JVI.80.2.941–950.2006

Monoclonal Antibodies Targeting the HR2 Domain and the Region Immediately Upstream of the HR2 of the S Protein Neutralize In Vitro Infection of Severe Acute Respiratory Syndrome Coronavirus

Kuo-Ming Lip,[1]† Shuo Shen,[1]*† Xiaoming Yang,[2] Choong-Tat Keng,[1] Aihua Zhang,[2] Hsueh-Ling Janice Oh,[1] Zhi-Hong Li,[1] Le-Ann Hwang,[1] Chih-Fong Chou,[1] Burtram C. Fielding,[1] Timothy H. P. Tan,[1] Josef Mayrhofer,[3] Falko G. Falkner,[3] Jianlin Fu,[1] Seng Gee Lim,[1] Wanjin Hong,[1] and Yee-Joo Tan[1]

Institute of Molecular and Cell Biology, Singapore 138673,[1] Wuhan Institute of Biological Products, Wuhan, P. R. China 430060,[2] and Baxter Vaccines, Orth/Donau, Austria[3]

Received 7 June 2005/Accepted 19 October 2005

We have previously shown that an *Escherichia coli*-expressed, denatured spike (S) protein fragment of the severe acute respiratory coronavirus, containing residues 1029 to 1192 which include the heptad repeat 2 (HR2) domain, was able to induce neutralizing polyclonal antibodies (C. T. Keng, A. Zhang, S. Shen, K. M. Lip, B. C. Fielding, T. H. Tan, C. F. Chou, C. B. Loh, S. Wang, J. Fu, X. Yang, S. G. Lim, W. Hong, and Y. J. Tan, J. Virol. 79:3289–3296, 2005). In this study, monoclonal antibodies (MAbs) were raised against this fragment to identify the linear neutralizing epitopes in the functional domain and to investigate the mechanisms involved in neutralization. Eighteen hybridomas secreting the S protein-specific MAbs were obtained. Binding sites of these MAbs were mapped to four linear epitopes. Two of them were located within the HR2 region and two immediately upstream of the HR2 domain. MAbs targeting these epitopes showed in vitro neutralizing activities and were able to inhibit cell-cell membrane fusion. These results provide evidence of novel neutralizing epitopes that are located in the HR2 domain and the spacer region immediately upstream of the HR2 of the S protein.

The virus-cell membrane fusion event is an essential step in the entry process of all enveloped animal viruses, including important human pathogens such as influenza virus, human immunodeficiency virus (HIV) (8, 23), and the newly emerged severe acute respiratory syndrome coronavirus (SARS-CoV) (9). Following the binding to their receptors on the cell surface, virus-encoded membrane fusion proteins mediate the fusion process. In many but not all cases, the viral fusion proteins are proteolytically processed by host proteases into 2 subunits that remain closely associated with each other: a surface subunit with a receptor-binding site and a transmembrane subunit with a fusion peptide consisting of two or more heptad repeat domains. Upon interaction of the fusion protein with a cellular receptor, the buried fusion peptide is exposed and inserted into the membrane of the target cell. A series of conformational changes trigger virus-cell fusion activity (9) and lead to the unloading of the viral genome into cells. Additionally, many viral fusion proteins also induce cell-cell fusion, i.e., the formation of multinucleated syncytia, facilitating the rapid spread of virus infection.

The spike (S) protein of coronaviruses is responsible for receptor binding and membrane fusion. It shares similarity with class I virus fusion proteins (2, 3). Typically, it is a type I integral membrane protein, which is N-glycosylated and trimerized in the endoplasmic reticulum. The N-terminal S1 protein contains the receptor-binding site (10, 18, 22, 34). The C-terminal S2 protein is a fusion subunit and anchors on the viral envelope through a transmembrane domain. The S2 protein ectodomain contains two 4,3 hydrophobic heptad repeats (HR1 and HR2) and a putative, internal fusion peptide (3, 23). For the SARS-CoV S protein, the HR2 is located adjacent to the transmembrane domain, whereas the HR1 is 140 to 170 residues upstream of the HR2.

Crystallographic, biophysical, and biochemical analysis of the fusion core of SARS-CoV S protein (2, 12, 19, 27, 30, 35) and other class I fusion proteins (8, 25) supports a model of membrane fusion probably adopted by these enveloped viruses. After the attachment of the receptor-binding subunit to the receptor, the HR1 and HR2 domains in the membrane fusion subunit interact with each other and form a six-helix bundle, a complex consisting of a homotrimeric HR1 coiled coil surrounded by three HR2 helices. The spacer domain (or link, or interhelical domain) between HR1 and HR2 forms a loop and reverses the direction of the polypeptide chain so that the HR2 helices pack against the HR1 coiled coil in an antiparallel manner. This conformational change results in a close apposition of the fusion peptide, already exposed and inserted into the target cellular membrane, with the viral transmembrane domain, leading to virus-cell membrane fusion. Obviously, the functional domains involved in membrane fusion are attractive targets for the discovery of viral entry inhibitors. Peptides derived from HR1 or HR2 can inhibit infection as shown for coronaviruses and many other viruses, presumably by

* Corresponding author. Mailing address: Institute of Molecular and Cell Biology, Proteos, 61 Biopolis Drive, Singapore 138673. Phone: 65 6586 9622. Fax: 65 67791117. E-mail: shenshuo@imcb.a-star.edu.sg.

† K.-M.L. and S.S. contributed equally to this article.

interfering with the formation of the six-helix bundle and inhibiting the initiation of membrane fusion. This strategy has been successfully used in the development of inhibitors for HIV infection (20). Potentially, monoclonal antibodies (MAbs) targeting fusion subunits might also inhibit the fusion in the same manner (21). For example, neutralizing MAbs against gp41 of HIV are likely to target fusion intermediates or epitopes that are exposed following receptor interactions (39, 41).

The S protein contains the determinants for host specificity, cell tropism, and pathogenesis. The S protein is also able to stimulate humoral and cellular immune responses (1, 6, 7, 13, 32), and therefore, it is one of the major targets for the development of vaccine candidates. Identification and characterization of neutralizing epitopes on S of SARS-CoV could provide useful leads to the development of efficacious vaccines (11, 26, 31, 37, 38). In our previous study (15), we have shown that an *Escherichia coli*-expressed fragment induces neutralizing polyclonal antibodies targeting domains involved in membrane fusion. In this study, monoclonal antibodies were generated using the same S fragment to determine the neutralizing antigenic sites in this region. The activities of in vitro neutralization and inhibition of cell-cell membrane fusion of the MAbs were tested in order to determine the mechanism involved in the neutralization of virus infectivity. The results showed that binding of MAbs to the functional domains might interfere with the interaction between the HR1 and HR2 domains required for membrane fusion and virus entry.

MATERIALS AND METHODS

Cells and viruses. Cos-7, CHO, Vero E6, and 293T cells were purchased from the American Type Culture Collection (Manassas, Va.) and were maintained in Dulbecco's modified Eagle medium (DMEM; Sigma-Aldrich Inc.) supplemented with 10% fetal calf serum (HyClone), streptomycin (1,000 μg/ml), and penicillin (1,000 U/ml). A CHO cell line (CHO-ACE2) stably expressing the receptor, ACE2, for SARS-CoV S was established using the methods described previously and grown in complete DMEM containing 0.1 mM $ZnSO_4$ (4). The strain Sin2774 of SARS-CoV (GenBank accession number AY283798) was isolated from a SARS patient in Singapore General Hospital and was adapted to grow in Vero E6 cells. Recombinant vaccinia/T7 virus (vTF7-3) was grown and titrated on Vero E6 cells. Recombinant vaccinia viruses rVV-L-SP and rVV-L-NP expressing the S and N proteins of SARS-CoV, respectively, were obtained from Baxter Vaccines and grown in CV-1 cells.

Construction of plasmids for expression in mammalian cells. A plasmid pKT-S containing the S gene of SARS-CoV was prepared as described previously (15). Specific primers were designed for two-round PCR to amplify S fragments with internal deletions of the S gene from nucleotide positions 3084 to 3150, 3151 to 3210, 3211 to 3270, 3271 to 3330, 3331 to 3390, 3391 to 3450, 3451 to 3510, and 3511 to 3576, respectively (numbering according to the S gene of strain Sin2774). The eight PCR products were digested with EcoRV and SacI and ligated to EcoRV/SacI-cut pKT-S under the control of a T7 promoter, giving rise to plasmids pKT-SΔ50, pKT-SΔ51, pKT-SΔ52, pKT-SΔ53, pKT-SΔ54, pKT-SΔ55, pKT-SΔ56, and pKT-SΔ57, respectively.

Generation of monoclonal antibodies. Glutathione *S*-transferase (GST)- and His-tagged fusion proteins GST-SΔ10 and SΔ10-His were expressed in *E. coli* and purified as described previously (15). They were used for immunization of mice and screening of hybridomas secreting S-specific MAbs, respectively. Each of the 6-week-old female BALB/c mice was given primary injection (intraperitoneal) with 100 μg of the protein GST-SΔ10 emulsified in complete Freund's adjuvant (Sigma-Aldrich Inc.). Two weeks later, each mouse was given one secondary booster injection using the same amount of antigen mixed with incomplete Freund's adjuvant (Sigma-Aldrich Inc.). Booster injections were administered to each mouse at 1-week intervals three more times. S-specific antibodies in the serum of immunized mice were tested by Western blot assays prior to hybridoma fusion. The spleen was excised, and hybridoma fusion was performed using the ClonalCell-HY Complete kit (StemCell Technologies, Canada) according to the manufacturer's instructions. All procedures on the use of laboratory animals were done in accordance with the regulations and guidelines of the National Advisory Committee for Laboratory Animal Research, Singapore. MAbs in supernatants of hybridoma cultures were screened in an enzyme-linked immunosorbent assay (ELISA). Briefly, 96-well ELISA plates were coated with the protein SΔ10-His or bovine serum albumin (50 ng/well) in 0.1 M sodium carbonate buffer (pH 9.6) overnight at 4°C. The plates were blocked with phosphate-buffered saline (PBS) containing 5% fetal calf serum and 0.05% Tween 20 for 1 h at 37°C and washed three times with PBS containing 0.05% Tween 20 and three times with PBS. Supernatants of hybridoma cultures (50 μl/well) were incubated for 1 h at 37°C. After washing, goat anti-mouse immunoglobulin G (IgG)-horseradish peroxidase antibodies (200 μg/ml, Santa Cruz, Calif.) at a dilution of 1:2,500 were added to the ELISA plates, which were then incubated for 1 h at 37°C. After washing three times with PBS, substrate TMB (Pierce Biotechnology) was added and the reaction was stopped 15 min later by adding an equal volume of 1 M H_2SO_4. Optical density was read at 450 nm. Mouse immune and preimmune sera were used as positive and negative controls. Samples giving a value of optical density that is equal or greater than 3 standard deviations above the mean value of bovine serum albumin controls were considered positive.

Western blot analysis of the S protein in transfected Cos-7 cells and infected Vero E6 cells. To prepare lysates of S-transfected cells, 50% of confluent monolayers of Cos-7 cells in 60-mm petri dishes was infected at a multiplicity of infection (MOI) of 1 with recombinant vaccinia virus vTF7-3 expressing bacteriophage T7 RNA polymerase. After 1 h of adsorption, cells were transfected with 2 to 4 μg of plasmid by using Effectene reagents (QIAGEN) according to the manufacturer's instruction. Transfected cells were incubated overnight at 37°C, and the cell lysate was prepared by resuspending the cell pellet in 1× protein sample buffer (60 mM Tris-HCl [pH 6.8], 1% sodium dodecyl sulfate [SDS], 20 mM dithiothreitol, 10% glycerol, 0.02% bromophenol blue). To prepare lysates of SARS-CoV-infected cells, confluent Vero E6 cells were infected with viruses at an MOI of 1 and were incubated at 37°C for 12 to 15 h. Cells were washed with PBS and were resuspended in lysis buffer containing 150 mM NaCl, 20 mM Tris (pH 7.5), 1% NP-40, 5 mM EDTA, and 1 mM phenylmethylsulfonyl fluoride. One volume of 5× standard protein sample buffer was added to 4 volumes of cell lysate. The samples were heated at 100°C for 5 min and were kept at −20°C before use. Proteins in cell lysates were separated by 10% polyacrylamide gel electrophoresis and transferred to a nitrocellulose membrane. The membranes were blocked in 5% nonfat milk in PBS with 0.05% Tween 20 and probed with either rabbit anti-SΔ10 serum (1:20,000) or MAbs (1:4,000) at 4°C overnight. The membranes were incubated with goat anti-rabbit or anti-mouse horseradish peroxidase-conjugated secondary antibodies (200 μg/ml; Santa Cruz) at a dilution of 1:2,000 for 1 h at room temperature and developed with enhanced chemiluminescence reagent (Pierce).

In vitro virus neutralization assay. Neutralization assays were performed in a 96-well plate format. Complement proteins in ascitic fluids were inactivated at 56°C for 30 min before use. MAbs were first diluted 10 times, and then serial twofold dilutions were prepared in maintenance medium. One set of antibody dilutions was added to cells to detect the toxicity of the ascitic fluids. The diluted antibodies were incubated with 10 50% tissue culture infective doses of SARS-CoV in an equal volume of medium for 1 h at 37°C before being added into the respective wells containing 5×10^4 Vero E6 cells per well. At each dilution, the mixtures of antibody and virus were added to four wells and incubated with Vero E6 cells. After 3 days, cytopathic effect (CPE) developed in all the negative controls and the back titration wells. The titers of the neutralizing antibodies were determined by applying the Kärber formula: Negative log of the lowest dilution − [(sum of percentage positive/100) − 0.5] × log interval. All experiments were carried out in triplicate, and the neutralizing titers were expressed as the reciprocal of the highest antibody dilution where the viral CPE in 50% of the wells was neutralized.

Fluorescence activated cell sorting (FACS) analysis. 293T cells infected with rVV-L-SP expressing the S proteins (293T-SP) and stable cell line CHO-ACE2 were first detached with 0.04% EDTA, washed once with PBS, and incubated with rabbit anti-SΔ10 serum diluted 1:40, MAbs or goat anti-ACE2 IgG primary antibodies (100 μg/ml; Santa Cruz) diluted 1:20 in PBS containing 1% fetal bovine serum and 0.1% sodium azide for 1 h at 4°C. Cells in tubes were placed on a roller to ensure constant mixing under nonpermeabilizing conditions. The cells were washed and subsequently incubated with fluorescein isothiocyanate (FITC)-labeled goat anti-rabbit IgG (200 μg/ml; Santa Cruz), rabbit anti-goat IgG secondary antibodies (200 μg/ml; Santa Cruz), or goat anti-mouse IgG secondary antibodies (200 μg/ml; Santa Cruz) at a 1:20 dilution for 1 h at 4°C and placed on a roller to ensure constant mixing. Immediately after washing, cells were measured for FITC fluorescence using a Becton Dickinson FACScan flow cytometer and results were analyzed using Cellquest Pro software.

Cell-cell membrane fusion assay. The 293T effector cells were transfected with plasmid pEGFP-N1 (Clontech Laboratories Inc, Pala Alto, Calif.), which encodes GFP, using Effectene transfection reagent (QIAGEN) according to the manufacturer's instructions. After 24 h, medium was removed and the cells were washed twice with room temperature PBS before the infection medium was added. Effector cells were infected with recombinant vaccinia virus expressing the SARS-CoV spike protein (rVV-L-SP) at an MOI of 0.1. After 1 h of adsorption, the infection medium was removed and subsequently replaced with complete DMEM for 24 h for S expression. The effector cells and target cells (CHO-ACE2) were first detached with 0.04% EDTA, washed once with PBS, and resuspended in DMEM containing 0.25 mg/ml porcine trypsin (JRH Biosciences Inc.) and 5.6% fetal bovine serum. Target and effector cells were mixed at a 1:1 ratio per well (up to 1×10^6 cells) in a 12-well plate (Nunc). Syncytium formation was observed 6 h after mixing of cells.

Inhibition of syncytium formation. Effector and target cells were prepared as described above. Serially diluted rabbit anti-SΔ10 serum (at a dilution factor of 1:40, 1:80, 1:160), preimmune serum (at a dilution factor of 1:40), or serially diluted MAbs (at dilution factor of 1:40, 1:80, 1:160) were preincubated with effector cells at 37°C for 10 min. To maintain the same antibody concentration used in the preincubation, more antibodies were added together with the target cells to the fusion medium to complete the cell-cell membrane fusion assay. Inhibition of syncytium formation could be observed from 6 h onwards. Five micrographs were taken randomly in a 10× magnified field of view on an Olympus UV microscope CKX41 equipped with an Olympus Camedia C-5060 digital camera. Syncytium with a size equal to or greater than 10 cells was considered a true fusion, and the average numbers of syncytia were scored. The total number (T) of possible syncytia without cell-cell membrane fusion inhibition was derived from fusion experiment with non-SARS-CoV-related mouse ascitic fluid (anti-dengue MAb serotype I 6F8-3) or rabbit preimmune serum. The number (I) of syncytia with inhibition effect was derived from fusion experiments in the presence of specific antibodies of interest. Percent inhibition of cell-cell membrane fusion was expressed as (T−I)/T.

RESULTS

Generation of monoclonal antibodies against SΔ10 region. Our previous work showed that an S region covering the entire HR2 domain and its upstream region induced neutralizing polyclonal antibodies in immunized animals, which might bind to linear epitopes (15). To identify linear neutralizing epitopes and characterize functional domains in this region, monoclonal antibodies were generated against the region covering residues 1029 to 1192 of the S protein. By using bacterially synthesized S fragment GST-SΔ10 (15) as an antigen, BALB/c mice were immunized and then boosted up to four times. Sera were collected 1 week after booster injections were given and tested for the presence of specific antibodies by Western blot assays. An antibody response was observed after the first booster injection was given (at a serum dilution of 1:1,000) (data not shown), indicating that the GST-SΔ10 fragment was highly immunogenic in terms of inducing antibodies in mice. After hybridoma fusion and hypoxyanthine-aminopterin-thymidine selection, culture supernatants of individual clones were screened by ELISA using a C-terminally His-tagged S fragment (SΔ10-His) covering the same region of S. This helped to eliminate clones that were reacting to GST antigenic determinants. Among 125 ELISA-positive hybridomas, 94 (75%) were positive in Western blot screening using the full-length S protein prepared in a vaccinia-T7 expression system in Cos-7 cells (15). These hybridomas were passaged twice, and the supernatants were retested in Western blot assays. The results indicated that 48 out of 94 (51%) hybridomas were stably secreting specific monoclonal antibodies. Among them, 18 hybridomas (37.5%) produced a higher concentration of MAbs in supernatants, which were used for the mapping of binding sites. Eight out of the 18 hybridomas (44%) were subcloned and used to generate ascitic fluids, which were characterized in neutralizing and membrane fusion blocking assays as described below.

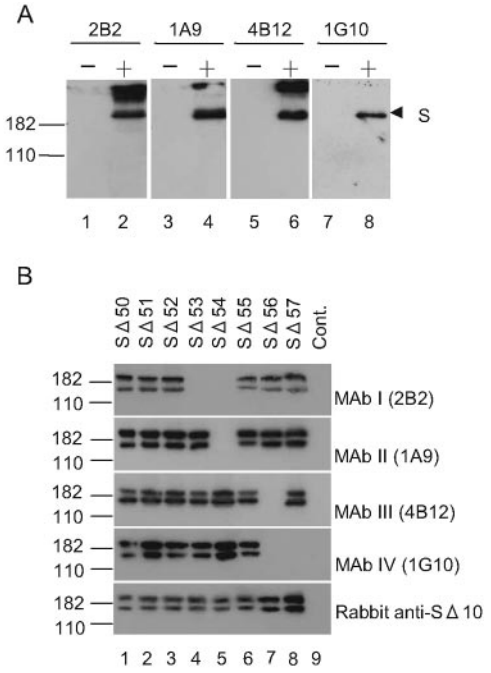

FIG. 1. (A) Detection of the S protein in virus-infected Vero E6 cells. Vero E6 cells were infected with SARS-CoV at an MOI of 1 (lanes 2, 4, 6, and 8) or mock infected (lanes 1, 3, 5, and 7) for 24 h. Cell lysates were separated on SDS–10% polyacrylamide gels and analyzed in Western blots using MAbs 2B2, 1A9, 4B12, and IG10. Molecular weight markers are indicated to the left. Position of the S protein is indicated by an arrowhead to the right. (B) Mapping of binding sites of monoclonal antibodies. The S mutant proteins (lanes 1 to 8, SΔ50 to SΔ57) with an internal 20- or 22-residue deletion were synthesized in a vaccinia-T7 expression system in Cos-7 cells. Cell lysates were separated on SDS–10% polyacrylamide gels and analyzed in Western blots using type I, II, III, and IV monoclonal antibodies and polyclonal antibody rabbit α-SΔ10 as indicated to the right of the gels. Mock-transfected cell lysate (lane 9) was used as a negative control (Cont.). Molecular weight markers are indicated to the left.

Detection of the S protein in SARS-CoV-infected cells by monoclonal antibodies. To confirm the binding specificity of MAbs to the S protein, all monoclonal antibodies were used to detect the S protein in virus-infected Vero E6 cells. Representative gels are shown in Fig. 1A. The MAbs could detect the 210-kDa S protein in infected (lanes 2, 4, 6, and 8) but not in mock-infected (lanes 1, 3, 5, and 7) cells. The results demonstrated that the monoclonal antibodies were specifically binding to the S protein in SARS-CoV-infected cells. The MAbs against the SΔ10 region recognize the full-length S protein synthesized in virus-infected Vero E6 cells, consistent with previous results (15) obtained using rabbit anti-SΔ10 polyclonal antibodies.

Mapping of binding sites of monoclonal antibodies. To determine the binding sites of the MAbs, eight internal deletion mutant plasmids were constructed, expressed in Cos-7 cells, and used to determine the linear binding sites of MAbs by Western blot analysis. Each of these mutants encodes an S protein with a 20- or 22-residue deletion (20 to 22 residues shorter than the full-length S protein). The positions of the

TABLE 1. Reactivity of MAbs against the internal-deletion S mutants

Mutant protein	Residues deleted	MAb type[a]			
		I	II	III	IV
SΔ50	1029–1050	+	+	+	+
SΔ51	1051–1070	+	+	+	+
SΔ52	1071–1090	+	+	+	+
SΔ53	1091–1110	−	+	+	+
SΔ54	1111–1130	−	−	+	+
SΔ55	1131–1150	+	+	+	+
SΔ56	1151–1170	+	+	−	−
SΔ57	1171–1192	+	+	+	−

[a] +, MAb binds to protein; −, MAb does not bind protein.

TABLE 3. In vitro neutralizing activities of MAbs

MAb	MAb type	Isotype	Titers	IgG (μg/ml)
2B2	I	IgG1	40	50
2G2	I	IgG1	47	85
1A9	II	IgG1	28	35
1C6	III	IgG1	24	83
1H1	III	IgG1	40	100
6B9	III	IgG1	24	42
4B12	III	IgG1	47	42
1G10	IV	IgG1	75	13
7G12		IgG1	0	50
Anti-dengue		IgG1	0	50

deleted amino acid residues are indicated in Table 1. The binding sites of MAbs from 18 hybridomas were mapped, and the results were shown by representative gels in Fig. 1B. In transfected cells, the unglycosylated form of S was produced (15). Both glycosylated and unglycosylated forms (bottom gel, lanes 1 to 8) of each mutant protein (SΔ50 to SΔ57) were detected using rabbit anti-SΔ10 serum. These were S-specific proteins, as no bands were detected in mock-transfected cells (lane 9). In contrast, S proteins encoded by one or two mutant constructs were not detected by each of the four types of MAbs; therefore, these MAbs bound to residues that were deleted in the corresponding internal-deletion mutants. As summarized in Table 2, 18 MAbs bound to four distinct antigenic sites and therefore were classified into types I (6 of 18), II (4 of 18), III (5 of 18), and IV (3 of 18). The type I, II, III, and IV MAbs bound to residues 1091 to 1130, 1111 to 1130, 1151 to 1170, and 1151 to 1192, respectively. The results showed that residues 1091 to 1192 of the SΔ10 fragment harbor the major antigenic epitopes, but not the residues 1029 to 1090. Antigenic site I (1091 to 1130) overlapped with site II (1111 to 1130), while antigenic site III (1151 to 1170) overlapped with site IV (1151 to 1192). Despite the overlap, each site was distinct from the other. It seems that these antigenic sites were immunodominant within the SΔ10 region (residues 1029 to 1192).

In vitro neutralization of virus infectivity by MAbs. Ascitic fluids of eight MAbs, all of which are of the immunoglobulin isotype 1, were prepared, and antibody concentrations of crude preparations were determined (Table 3). The ascitic fluids were diluted 10 times, and then serial twofold dilutions were prepared. Neutralization assays were performed in a 96-well plate format by incubating equal volumes of diluted antibodies and virus suspension containing 10 50% tissue culture infective doses for 1 h at 37°C and then adding the mixtures to confluent Vero E6 cells in wells. After 3 days, complete CPE was observed in all control wells containing virus suspension in the absence of antibodies of interest and in wells containing anti-dengue MAb (non-SARS-CoV related) or a nonneutralizing MAb, 7G12-6, targeting amino acid residues 281 to 300 of S. Ascitic fluids were not cytotoxic at the starting concentration used. The neutralizing titers were expressed as the reciprocal of the final dilution of antibodies required to completely protect cells in 50% of the wells (no CPE was observed) from virus infection. As shown in Table 3, all four types of MAbs showed neutralizing activities with titers ranging from 24 to 75 at MAb concentrations ranging from 13 to 100 μg/ml. The results showed that the amino acid residues, which the MAbs bound to, might represent the neutralizing epitopes on the S protein.

TABLE 2. Binding sites

Binding site	Mab type	% of hybridomas (no./total no.)
1091–1130	I	33.3 (6/18)
1111–1130	II	22.2 (4/18)
1151–1170	III	27.7 (5/18)
1151–1192	IV	16.6 (3/18)

Neutralizing MAbs binding to regions upstream of and within the HR2 domain. The amino acid sequence of the region (residues 1091 to 1192), which the four types of monoclonal antibodies target, were aligned with those of the corresponding S regions of other coronaviruses (Fig. 2). The HR2 domain of the SARS-CoV S protein has been predicted to be located within residues 1125 to 1193 or 1144 to 1191 (3, 35). Therefore, the upstream region from residues 1091 to 1124 or 1143 is considered a part of the spacer region between HR1 and HR2. As shown in Fig. 2, type I and II MAbs bound to the spacer region immediately upstream of HR2, residues 1091 to 1131 and 1111 to 1131, respectively. Type III and IV MAbs bound directly to the HR2 domain (residues 1151 to 1192). As indicated in Fig. 2, these neutralizing epitopes on SARS-CoV S protein were different from the amino acid residues SIAPD LSLDFEKLNV (shown by a line with arrows at the both ends) bound by the neutralizing MAb of the murine hepatitis virus (MHV) S protein characterized previously (21). The results suggested that the HR2 domain and the spacer region immediately upstream of HR2 harbored neutralizing epitopes and therefore might be functionally important domains.

Inhibition of S-induced cell-cell membrane fusion by MAbs. During the virus entry into cells, the HR1 and HR2 domains interact with each other and a subsequent conformational change triggers virus-cell membrane fusion. To test if the antibodies targeting this functional region could interfere with the HR1 and HR2 interaction and block membrane fusion, a cell-cell membrane fusion assay was developed. Effector cells, 293T, infected with rVV-L-SP, expressing S proteins (293T-SP), and the target cells, CHO-ACE2, expressing receptor ACE2, were used to achieve this end.

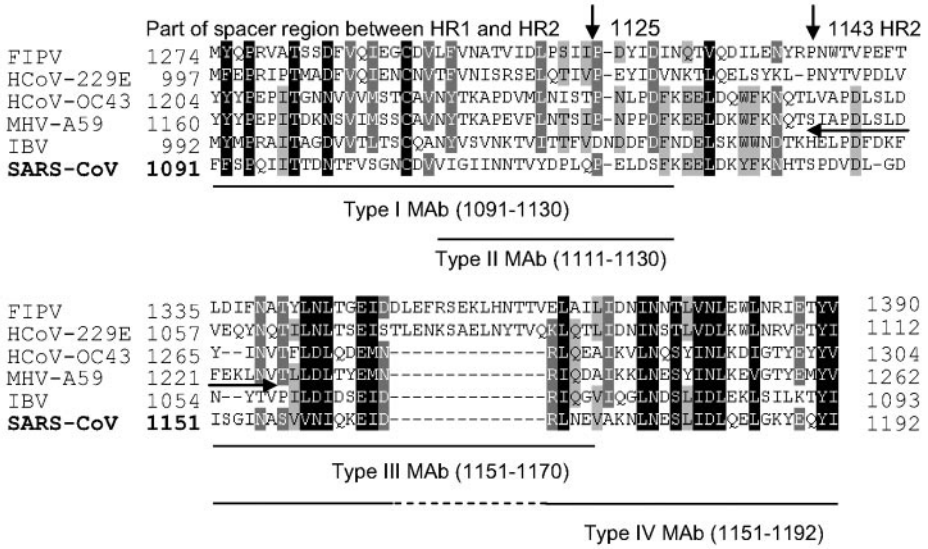

FIG. 2. Clustal W multiple sequence alignment of coronavirus S proteins. The S region corresponding to the binding sites of monoclonal antibodies to SARS-CoV (Singapore strain 2774) is aligned with those of the group 1 coronaviruses feline infectious peritonitis virus (FIPV) and human coronavirus 229E (HCoV-229E), the group 2 coronaviruses HCoV-OC43 and MHV-59A (mouse hepatitis virus), and the group 3 coronavirus infectious bronchitis virus (IBV) (GenBank accession numbers AY283798, VGIH79, VGIHHC, CAA83661, VGIH59, and M95169, respectively). The shading indicates sequence identity and similarity. The predicted HR2 region and upstream spacer region and binding sequences of type I, II, III, and IV monoclonal antibodies are shown by arrows and lines. The line with arrows at both ends represents the binding site of a neutralizing MAb against S of MHV (23).

First, FACS analysis was performed to verify that the S and ACE2 proteins were expressed on the cell surface of 293T-SP and CHO-ACE2 cells, respectively, under nonpermeabilizing conditions. 293T-SP cells were incubated with rabbit anti-SΔ10 primary antibodies, and CHO-ACE2 cells were incubated with goat anti-ACE2 primary antibodies. The cells were subsequently incubated with FITC-conjugated goat anti-rabbit or rabbit anti-goat IgG secondary antibodies. As shown in Fig. 3A (left), FITC fluorescence intensity measured for CHO-ACE2 was higher than that for control cells CHO, indicating expression of ACE2 proteins on the surface of CHO-ACE2 cells. As shown in Fig. 3A (right), FITC fluorescence measured for 293T-SP was higher than that for control cells 293T-NP expressing the N (nucleocapsid) protein of SARS-CoV. In another parallel FACS experiment, rabbit anti-SΔ10 or preimmune serum was incubated with 293T-SP and FITC fluorescence intensity measured for rabbit anti-SΔ10 was significantly higher than that for control preimmune serum (data not shown). These results indicated that S was presented on the cell surface.

To investigate if the epitopes upstream of HR2 (types I and II) and within HR2 (types III and IV) are exposed and accessible to specific antibodies, eight MAbs of interest (1:20) or an unrelated anti-dengue MAb was incubated with the effector cells, 293T-SP. The cells were subsequently incubated with FITC-conjugated goat anti-mouse IgG secondary antibodies. The interaction between the MAbs and S was measured by FACS analysis. In Fig. 3B, a representative histogram of each type of MAb (type I MAb, 2B2; type II MAb, 1A9; type III MAb, 4B12; type IV MAb, 1G10) is shown. Generally, FITC fluorescence intensity measured for each MAb was significantly higher than that for control anti-dengue MAb. This indicated that the eight MAbs could bind to the four epitopes on S and that these epitopes on the S proteins were exposed and accessible to specific antibodies.

Next, a cell-cell membrane fusion assay was set up for syncytium formation. Effector cells, 293T-SP or 293T-NP, transfected with pEGFP-N1 (expressing green fluorescent protein [GFP]) were incubated with either target CHO-ACE2 or normal CHO cells. All cell-cell membrane fusion experiments were done in triplicate. A representation of the morphology of normal cells and cells that have undergone cell-cell fusion is shown in Fig. 3C. As seen in the top row, syncytium formation with 10 or more cells fused together as a result of the interaction between S and ACE2, which were expressed on the surfaces of effector cells, 293T-SP, and target cells, CHO-ACE2, was displayed in a bright field (left), a dark field under UV excitation (right), and a combined view (center). In contrast, no syncytium was observed when control effector cells, 293T-NP, were incubated with CHO-ACE2 (Fig. 3C, bottom micrographs). In Fig. 3C (bottom micrographs), individual cells were well distinguishable with a clear cell boundary in the bright field (left) and as single spots of green fluorescence in the dark field (right), in contrast to the lack of cell boundaries and massive bodies of green fluorescence as shown in Fig. 3C, top micrographs. 293T-SP incubated with normal CHO cells did not yield any syncytia in the fusion experiments (data not shown). Only fusion experiments consisting of effector cells, 293T-SP, and target cells, CHO-ACE2, could form syncytia. These results confirmed that the cell-cell membrane fusion assay was induced by S and was dependent on the receptor ACE2 (18, 24, 26).

In order to investigate the inhibition of syncytium formation by specific antibodies, the four types of MAbs comprised of 8 MAbs (2B2 and 2G2 in type I; 1A9 in type II; 1C6, 1H1, 4B12, and 6B9 in type III; and 1G10 in type IV), a non-SARS-CoV-

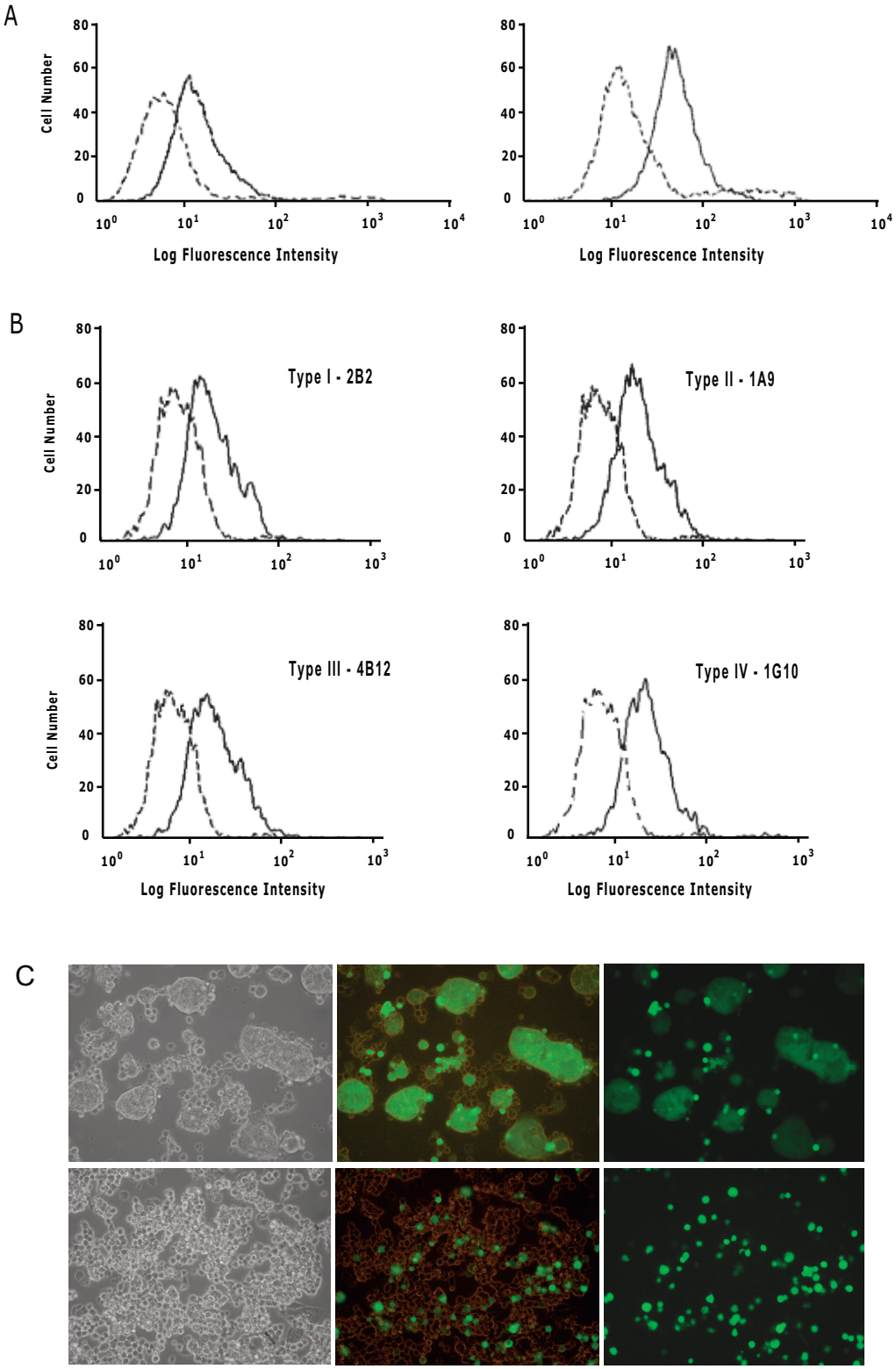

FIG. 3. (A) FACS analysis of the surface expression of the S and ACE2 proteins. Left, ACE2 surface expression on CHO-ACE2 stable cells (solid line) and negative control CHO cells (dotted line) was probed with goat anti-ACE2 primary and FITC-conjugated anti-goat IgG secondary antibodies. Right, S protein surface expression (solid line) and nucleocapsid protein expression (dotted line; negative control) on 293T cells was probed with rabbit anti-SΔ10 primary and FITC-conjugated anti-rabbit IgG secondary antibodies. (B) FACS analysis of the four epitopes located upstream of HR2 and within HR2 on S. Effector cells, 293T-SP, were probed with four representative MAbs of interest and an unrelated anti-dengue MAb, followed by FITC-conjugated anti-mouse IgG secondary antibodies. Top left panel, S was probed with type I MAb 2B2 (solid line) and anti-dengue MAb (dotted line). Top right panel, S was probed with type II MAb 1A9 (solid line) and anti-dengue MAb (dotted line).

related anti-dengue MAb, rabbit anti-SΔ10 serum, or rabbit preimmune serum and goat anti-ACE2 antibody were incubated in the cell-cell membrane fusion assay at 1:40, 1:80, and 1:160 dilutions, respectively. Rabbit anti-SΔ10 serum and goat anti-ACE2 antibody were included as positive controls, and rabbit preimmune serum and anti-dengue MAb were included as negative controls. Representative micrographs of syncytium formation between effector and target cells are shown in Fig. 4A. Syncytium formation was not observed in the presence of 1:40 diluted rabbit anti-SΔ10 serum (top right) or MAb 1A9 (bottom right). No syncytium formation was observed in the presence of goat anti-ACE2 antibody (data not shown). In contrast, as shown in the left panels, large syncytia were observed in the presence of 1:40 noninhibiting rabbit preimmune serum (top left) or anti-dengue MAb (bottom left).

Next, the distribution of the number of nuclei per syncytium was scored. It was found that syncytia formed from 10 or more cells accounted for at least 90% of all potential syncytia scored (data not shown). Only syncytia with 10 nuclei or more were counted in order to eliminate artifacts scored as a result of cell division or abnormal cell clumping and to avoid difficulty in determining syncytia of small size. This formed the basis for scoring true fusion for subsequent cell-cell fusion assays.

The number of syncytia was then scored, and the percentage of the syncytium inhibition at different antibody dilutions is summarized in Fig. 4B. At a 1:40 dilution, all the MAbs inhibited more than 50% of syncytium formation. However, syncytia inhibition decreased significantly when each MAb was serially diluted from 1:40 to 1:80 and 1:160. The formation of syncytia was inhibited in a dose-dependent manner, indicating that the MAbs were specific in blocking cell-cell membrane fusion.

DISCUSSION

An attractive approach to interfere with viral infection and prevent SARS is to block the virus-cell membrane fusion using inhibitory drugs (peptides or nonpeptides) or neutralizing antibodies binding to domains involved in membrane fusion. Peptides derived from the HR1 or HR2 domains of viral fusion glycoproteins can effectively inhibit virus infections caused by retroviruses, paramyxoviruses, and coronaviruses (3, 14, 17, 33). It has been demonstrated that peptides derived from the HR2 domain of S could inhibit the in vitro replication of SARS-CoV, although less effectively than the similar peptides against the S protein of MHV (3). Binding sites of several neutralizing MAbs were mapped to linear epitopes on S2 of MHV 59A and predicted to form a coiled coil and to be involved in membrane fusion (8). In this study, an S fragment was used to immunize mice, as it could induce neutralizing polyclonal antibodies (15). MAbs were generated and analyzed by Western blot using S deletion mutants. Binding sites of the MAbs were mapped to linear epitopes on the HR2 domain and to the spacer region between the HR1 and HR2 domains. Using these MAbs, we could investigate the mechanism of membrane fusion and virus entry.

In our previous study, the SΔ10 region from residues 1029 to 1192 induced neutralizing antibodies (15). As another S fragment (SΔ9, residues 798 to 1054) containing the residues 1029 to 1054 did not induce neutralizing antibodies, the residues 1055 to 1192 were considered to contain the neutralizing region. In this study, all the 18 MAbs raised against SΔ10 targeted the sites downstream of residue 1091 but not the region upstream of residue 1091. These results suggested that antigenic sites (I, II, III, and IV) recognized by these MAbs might be immunodominant in humoral immunity to SΔ10. The neutralizing region has been narrowed down to residues 1091 to 1130 and 1151 to 1192, as the region contained the predominant antigenic sites.

Our results have shown that MAbs targeting the linear epitopes on the fusion core of the S2 region of SARS-CoV were able to neutralize virus infectivity, consistent with results obtained from the previous work using polyclonal antibodies (15). The neutralizing titers of these MAbs against membrane fusion domains were relatively low compared with the MAbs against the receptor-binding domain of the SARS S protein (5, 26). However, the results were consistent with previous findings on murine coronavirus that the neutralizing titers of MAbs against membrane-fusion S2 were 3 to 4 orders of magnitude lower than those against the receptor-binding S1 region (16, 28). In another study, the binding site of a MAb was mapped to the HR2 domain and the neutralizing titer was 32 times lower than a MAb against the receptor-binding site of MHV (40 versus 1,280) (21). The different neutralizing titers obtained might be due to the accessibility of the respective determinants on the S1 and S2 subunits of mature virions. Nevertheless, anti-SΔ10 polyclonal antibodies against multiple epitopes do neutralize virus infection more efficiently than each of these MAbs (targeting a single epitope). It remains to be investigated if the polyclonal antibodies act cooperatively or synergistically (40).

Overall, the results of syncytium inhibition by the eight MAbs were consistent with the results obtained from the virus neutralization assays. Specific MAbs that could inhibit syncytium formation could also protect cells against in vitro virus infection. An interesting observation was the less-effective neutralizing property of MAb 1A9 despite its effectiveness at cell-cell membrane blocking. The reason for this is not clear and needs further investigation.

The structure of the fusion core of the SARS-CoV S protein has been determined, demonstrating that residues 1150 to 1184 in HR2 interacted with residues 902 to 947 of HR1 (27, 35). Biophysical and biochemical analysis also revealed that residues 1142 to 1188 of HR2 interacted with residues 896 to 972 of HR1 (12). Furthermore, another study showed that the interaction domains

Bottom left panel, S was probed with type III MAb 4B12 (solid line) and anti-dengue MAb (dotted line). Bottom right panel, S was probed with type IV MAb 1G10 (solid line) and anti-dengue MAb (dotted line). (C) Syncytium formation between effector and target cells shown in a bright field (left panel), a dark field (right panel), and a combination of both (center panel). Top panel, effector cells 293T expressing S and GFP were mixed with target cells CHO-ACE2 expressing the ACE2 protein. Bottom panel, effector cells 293T expressing N and GFP were mixed with target cells CHO-ACE2 expressing ACE2 protein. Micrographs were taken at a magnification of ×20.

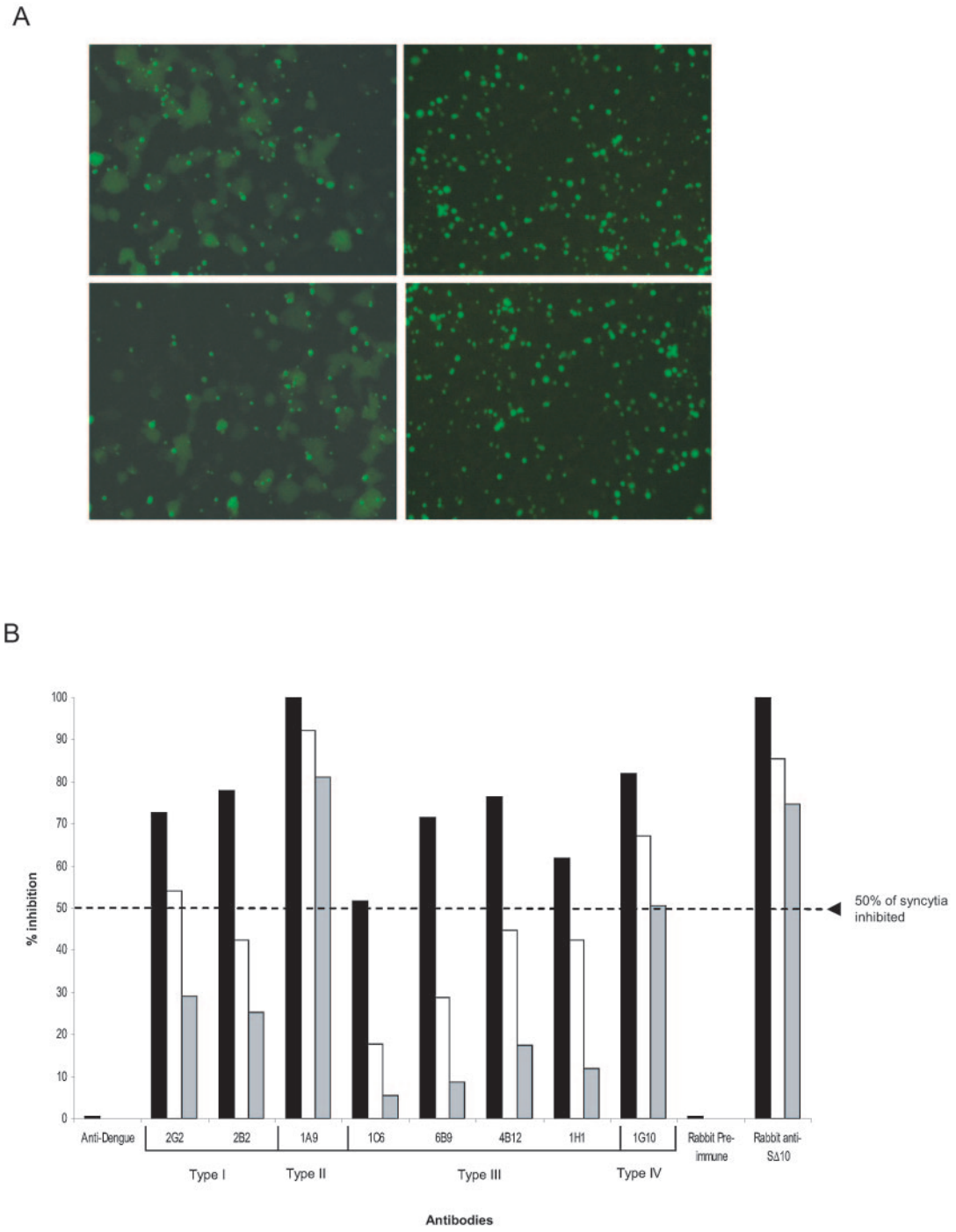

FIG. 4. (A) Inhibition of syncytium formation between effector and target cells. Top panel, incubation with rabbit preimmune serum (left) and rabbit anti-S10 polyclonal antibody (right) at 1:40 dilution. Bottom panel, incubation with mouse anti-dengue ascitic fluid (left) and mouse MAb 1A9 (right) at a 1:40 dilution. Micrographs were taken at a magnification of ×10. (B) Dose-dependent inhibition of syncytium formation between effector cells, 293T-SP, expressing S and target cells, CHO-ACE2, expressing ACE2 in the presence of antibodies at 1:40 (black), 1:80 (white), and 1:160 (gray) dilutions.

were mapped to residues 1151 to 1185 of HR2 and residues 916 to 950 of HR1 (30). Evidence shows that HR1 and HR2 form a six-helix bundle, a structure also observed for other type 1 viral fusion proteins in their fusion-competent state. The type III and IV MAbs also bound to these residues in the HR2 domain (residues 1151 to 1170 and 1151 to 1192, respectively) as described above. Therefore, it is reasonable to assume that the binding of antibodies to this region upset the interaction of HR1 and HR2, interfered with the conformational changes, and abolished the fusion activity. A previous study showed that a neu-

tralizing MAb against the S protein of MHV bound to a linear epitope (SIAPDLSLDFEKLNV) (Fig. 2) located within the HR2 domain (21). This MAb also blocked membrane fusion, indicating that the mechanism involved in neutralization by these MAbs is the blocking of virus-cell membrane fusion. Interestingly, type III and IV MAbs also bound to the HR2 domain and display neutralizing and cell-cell fusion inhibition properties. Our results are consistent with previous studies showing that the peptides mimicking residues 1161 to 1187 (HR2-18) (36), 1153 to 1189 (CP1) (19), 1126 to 1193 (sHR2-8), and 1130 to 1189 (sHR2-2) (3) of the HR2 inhibit the propagation of SARS-CoV. These could interact with the HR1 region, interfere with the formation of the six-helix bundle, and inhibit membrane fusion.

The type I and II MAbs bound to the sites (residues 1091 to 1130) upstream of residue 1131, which is immediately upstream of the HR2 domain beyond the boundaries of the extended conformation and α-helix of the HR2 domain determined previously (12, 30, 35). The neutralizing mechanism of type I and II MAbs is unknown. It is likely that the occupancy of the spacer region between the HR1 and HR2 by a MAb interferes with the interaction of these two domains by steric hindrance. If this is the case, our results indicated that the spacer region, especially the domain immediately upstream of the HR2 domain, plays an important role in mediating HR1/HR2 interaction, conformational change, and membrane fusion. The longer spacer region (about 140 to 170 residues) between the HR1 and HR2 domains is one of the unique characteristics of the S protein of CoV, similar to the paramyxovirus SV5 F1 protein (250 residues), but different from fusion proteins of other enveloped viruses (5 to 26 residues) (2). It is believed that the absence of a spacer region or a very short region between the HR2 and transmembrane domains is compensated for by the presence of a large spacer region between the HR1 and HR2 domains (12). The spacer region might provide the flexibility to form a loop so that the trimeric HR1 coiled coil could be packed with the three helices of the HR2 in an anti-parallel manner during the six-helix bundle formation.

The identification of these novel neutralizing sites could lead to the development of efficacious vaccines based on peptide mimics of the linear epitopes. Furthermore, the spacer region identified in this study might provide a new target for the development of entry inhibitors. Subunit vaccine candidates (including HR2 and the spacer region), derived from the neutralizing epitopes identified in this study, could be designed and tested in animal models for potential usage in the prevention of SARS-CoV infection. Previous work has shown that a decapeptide homologous to residues 993 to 1002 of the S protein of murine hepatitis virus strain JHM, located near the HR1 domain and between the HR1 and HR2 domains, elicited high levels of neutralizing antibody and protected mice against lethal virus challenge (29). Recently, a study showed that a peptide derived from residues 1167 to 1175 within the HR2 domain of the SARS-CoV S protein could elicit specific immune responses mediated by cytotoxic T lymphocytes (32). Thus, molecular dissection of the HR2 domain may finally help to understand the mechanisms of immune responses and drug inhibition.

ACKNOWLEDGMENTS

We thank Tham Puay Yoke, Choi Yook-Wah, Chan Zhen Li Daphne, Vithiagaran Gunalan, Xu Qiurong, Bi Lan, Li Pingping, and Zhizheng Fang for technical assistance.

This work was supported by a grant from the Agency for Science, Technology and Research (A-STAR), Singapore.

REFERENCES

1. **Bergmann, C. C., Q. Yao, M. Lin, and S. A. Stohlman.** 1996. The JHM strain of mouse hepatitis virus induces a spike protein-specific Db-restricted cytotoxic T cell response. J. Gen. Virol. **77:**315–325.
2. **Bosch, B. J., R. van der Zee, C. A. M. de Haan, and P. J. M. Rottier.** 2003. The coronavirus spike protein is a class I virus fusion protein: structural and functional characterization of the fusion core complex. J. Virol. **77:**8801–8811.
3. **Bosch, B. J., B. E. E. Martina, R. Van Der Zee, J. Lepault, B. J. Haijema, C. Versluis, A. J. Heck, R. De Groot, A. D. M. E. Osterhaus, and P. J. M. Rottier.** 2004. Severe acute respiratory syndrome coronavirus (SARS-CoV) infection inhibition using spike protein heptad repeat-derived peptides. Proc. Natl. Acad. Sci. USA **101:**8455–8460.
4. **Chou, C. F., S. Shen, Y. J. Tan, B. C. Fielding, T. H. P. Tan, J. Fu, Q. Xu, S. G. Lim, and W. Hong.** 2005. A novel cell-based binding assay system reconstituting interaction between SARS-CoV S protein and its cellular receptor. J. Virol. Methods **123:**41–48.
5. **Chou, T. H., S. Wang, P. V. Sakhatskyy, I. Mboudoudjeck, J. M. Lawrence, S. Huang, S. Coley, B. Yang, J. Li, Q. Zhu, and S. Lu.** 2005. Epitope mapping and biological function analysis of antibodies produced by immunization of mice with an inactivated Chinese isolate of severe acute respiratory syndrome-associated coronavirus (SARS-CoV). Virology **334:**134–143.
6. **Correa, I., G. Jimenez, C. Sune, M. J. Bullido, and L. Enjuanes.** 1988. Antigenic structure of the E2 glycoprotein from transmissible gastroenteritis coronavirus. Virus Res. **10**:77–93.
7. **Daniel, C., M. Lacroix, and P. J. Talbot.** 1994. Mapping of linear antigenic sites on the S glycoprotein of a neurotropic murine coronavirus with synthetic peptides: a combination of nine prediction algorithms fails to identify relevant epitopes and peptide immunogenicity is drastically influenced by the nature of the protein carrier. Virology **202:**540–549.
8. **Daniel, C., R. Anderson, M. J. Buchmeier, J. O. Fleming, W. J. Spaan, H. Wege, and P. J. Talbot.** 1993. Identification of an immunodominant linear neutralization domain on the S2 portion of the murine coronavirus spike glycoprotein and evidence that it forms part of complex tridimensional structure. J. Virol. **67:**1185–1194.
9. **Eckert, D. M., and P. S. Kim.** 2000. Mechanisms of viral membrane fusion and its inhibition. Annu. Rev. Biochem. **70:**777–810.
10. **Godet, M., J. Grosclaude, B. Delmas, and H. Laude.** 1994. Major receptor-binding and neutralization determinants are located within the same domain of the transmissible gastroenteritis virus (coronavirus) spike protein. J. Virol. **68:**8008–8016.
11. **Greenough, T. C., G. J. Babcock, A. Roberts, H. J. Hernandez, W. D. Thomas, Jr., J. A. Coccia, R. F. Graziano, M. Srinivasan, I. Lowy, R. W. Finberg, K. Subbarao, L. Vogel, M. Somasundaran, K. Luzuriaga, J. L. Sullivan, and D. M. Ambrosino.** 2005. Development and characterization of a severe acute respiratory syndrome-associated coronavirus-neutralizing human monoclonal antibody that provides effective immunoprophylaxis in mice. J. Infect. Dis. **191:**507–514.
12. **Ingallinella, P., E. Bianchi, M. Finotto, G. Cantoni, D. M. Eckert, V. M. Supekar, C. Bruckmann, A. Carfi, and A. Pessi.** 2004. Structural characterization of the fusion-active complex of severe acute respiratory syndrome (SARS) coronavirus. Proc. Natl. Acad. Sci. USA **101:**8709–8714.
13. **Jiménez, G., I. Correa, M. P. Melgosa, M. J. Bullido, and L. Enjuanes.** 1986. Critical epitopes in transmissible gastroenteritis virus neutralization. J. Virol. **60:**131–139.
14. **Joshi, S. B., R. E. Dutch, and R. A. Lamb.** 1998. A core trimer of the paramyxovirus fusion protein: parallels to influenza virus hemagglutinin and HIV-1 gp41. Virology **248:**20–34.
15. **Keng, C. T., A. Zhang, S. Shen, K. M. Lip, B. C. Fielding, T. H. Tan, C. F. Chou, C. B. Loh, S. Wang, J. Fu, X. Yang, S. G. Lim, W. Hong, and Y. J. Tan.** 2005. Amino acids 1055 to 1192 in the S2 region of severe acute respiratory syndrome coronavirus S protein induce neutralizing antibodies: implications for the development of vaccines and antiviral agents. J. Virol. **79:**3289–3296.
16. **Kubo, H., S. Takase-Yoden, and F. Taguchi.** 1993. Neutralization and fusion inhibition activities of monoclonal antibodies specific for the S1 subunit of the spike protein of neurovirulent murine coronavirus JHMV c1-2 variant. J. Gen. Virol. **74:**1421–1425.
17. **Lambert, D. M., S. Barney, A. l. Lambert, K. Guthrie, R. Medinas, D. E. Davis, T. Bucy, J. Erickson, G. Merutka, and S. R. Petteway, Jr.** 1996. Peptides from conserved regions of paramyxovirus fusion (F) proteins are potent inhibitors of viral fusion. Proc. Natl. Acad. Sci. USA **93**:2186–2191.
18. **Li, W., M. J. Moore, N. Vasilieva, J. Sui, S. K. Wong, M. A. Berne, M. Somasundaran, J. L. Sullivan, K. Luzuriaga, T. C. Greenough, H. Choe, and**

M. Farzan. 2003. Angiotensin-converting enzyme 2 is a functional receptor for the SARS coronavirus. Nature **426:**450–454.
19. **Liu, S., G. Xiao, Y. Chen, Y. He, J. Niu, C. R. Escalante, H. Xiong, J. Farmar, A. K. Debnath, P. Tien, and S. Jiang.** 2004. Interaction between heptad repeat 1 and 2 regions in spike protein of SARS-associated coronavirus: implications for virus fusogenic mechanism and identification of fusion inhibitors. Lancet **363:**938–947.
20. **Moore, J. P., and R. W. Doms.** 2003. The entry of entry inhibitors: a fusion of science and medicine. Proc. Natl. Acad. Sci. USA **100:**10598–10602.
21. **Routledge, E., R. Stauber, M. Pfleiderer, and S. G. Siddell.** 1991. Analysis of murine coronavirus surface glycoprotein functions by using monoclonal antibodies. J. Virol. **65:**254–262.
22. **Saeki, K., N. Ohtsuka, and F. Taguchi.** 1997. Identification of spike protein residues of murine coronavirus responsible for receptor-binding activity by use of soluble receptor-resistant mutants. J. Virol. **71:**9024–9031.
23. **Sainz, B., Jr., J. M. Rausch, W. R. Gallaher, R. F. Garry, and W. C. Wimley.** 2005. Identification and characterization of the putative fusion peptide of the severe acute respiratory syndrome-associated coronavirus spike protein. J. Virol. **79:**7195–7206.
24. **Simmons, G., J. D. Reeves, A. J. Rennekamp, S. M. Amberg, A. J. Piefer, and P. Bates.** 2004. Characterization of severe acute respiratory syndrome-associated coronavirus. Proc. Natl. Acad. Sci. USA **101:**4240–4245.
25. **Skehel, J. J., and D. C. Wiley.** 2000. Receptor binding and membrane fusion in virus entry: the influenza hemagglutinin. Annu. Rev. Biochem. **69:**531–569.
26. **Sui, J., W. Li, A. Murakami, A. Tamin, L. J. Matthews, S. K. Wong, M. J. Moore, A. S. Tallarico, M. Olurinde, H. Choe, L. J. Anderson, W. J. Bellini, M. Farzan, and W. A. Marasco.** 2004. Potent neutralization of severe acute respiratory syndrome (SARS) coronavirus by a human mAb to S1 protein that blocks receptor association. Proc. Natl. Acad. Sci. USA **101:**2536–2541.
27. **Supekar, V. M., C. Bruckmann, P. Ingallinella, E. Bianchi, A. Pessi, and A. Carfi.** 2004. Structure of a proteolytically resistant core from the severe acute respiratory syndrome coronavirus S2 fusion protein. Proc. Natl. Acad. Sci. USA **101:**17958–17963.
28. **Taguchi, F., and Y. K. Shimazaki.** 2000. Functional analysis of an epitope in the S2 subunit of the murine coronavirus spike protein: involvement in fusion activity. J. Gen. Virol. **81:**2867–2871.
29. **Talbot, P. J., G. Dionne, and M. Lacroix.** 1988. Vaccination against lethal coronavirus-induced encephalitis with a synthetic decapeptide homologous to a domain in the predicted peplomer stalk. J. Virol. **62:**3032–3036.
30. **Tripet, B., M. W. Howard, M. Jobling, R. K. Holmes, K. V. Holmes, and R. S. Hodges.** 2004. Structural characterization of the SARS-coronavirus spike S fusion protein core. J. Biol.Chem. **279:**20836–20849.
31. **van den Brink, E. N., J. Ter Meulen, F. Cox, M. A. Jongeneelen, A. Thijsse, M. Throsby, W. E. Marissen, P. M. Rood, A. B. Bakker, H. R. Gelderblom, B. E. Martina, A. D. Osterhaus, W. Preiser, H. W. Doerr, J. de Kruif, and J. Goudsmit.** 2005. Molecular and biological characterization of human monoclonal antibodies binding to the spike and nucleocapsid proteins of severe acute respiratory syndrome coronavirus. J. Virol. **79:**1635–1644.
32. **Wang. B., H. Chen, X. Jiang, M. Zhang, T. Wan, N. Li, X. Zhou, Y. Wu, F. Yang, Y. Yu, X. Wang, R. Yang, and X. Cao.** 2004. Identification of an HLA-A*0201-restricted CD8+ T-cell epitope SSp-1 of SARS-CoV spike protein. Blood **104:**200–206.
33. **Wild, C. T., D. C. Shugars, T. K. Greenwell, C. B. McDanal, and T. J. Matthews.** 1994. Peptides corresponding to a predictive alpha-helical domain of human immunodeficiency virus type 1 gp41 are potent inhibitors of virus infection. Proc. Natl. Acad. Sci. USA **91:**9770–9774.
34. **Wong, S. K., W. Li, M. J. Moore, H. Choe, and M. Farzan.** 2004. A 193-amino acid fragment of the SARS coronavirus S protein efficiently binds angiotensin-converting enzyme 2. J. Biol. Chem. **279:**3197–3201.
35. **Xu, Y., Y. Liu, Z. Lou, L. Qin, X. Li, Z. Bai, H. Pang, P. Tien, G. F. Gao, and Z. Rao.** 2004. Structural basis for coronavirus-mediated membrane fusion. Crystal structure of mouse hepatitis virus spike protein fusion core. J. Biol. Chem. **279:**30514–30522.
36. **Yuan, K., L. Yi, J. Chen, X. Qu, T. Qing, X. Rao, P. Jiang, J. Hu, Z. Xiong, Y. Nie, X. Shi, W. Wang, C. Ling, X. Yin, K. Fan, L. Lai, M. Ding, and H. Deng.** 2004. Suppression of SARS-CoV entry by peptides corresponding to heptad regions on spike glycoprotein. Biochem. Biophys. Res. Commun. **319:**746–752.
37. **Zhong, X., H. Yang, Z. F. Guo, W. Y. Sin, W. Chen, J. Xu, L. Fu, J. Wu, C. K. Mak, C. S. Cheng, Y. Yang, S. Cao, T. Y. Wong, S. T. Lai, Y. Xie, and Z. Guo.** 2005. B-cell responses in patients who have recovered from severe acute respiratory syndrome target a dominant site in the S2 domain of the surface spike glycoprotein. J. Virol. **79:**3401–3408.
38. **Zhou, T., H. Wang, D. Luo, T. Rowe, Z. Wang, R. J. Hogan, S. Qiu, S., R. J. Bunzel, G. Huang, V. Mishra, T. G. Voss, R. Kimberly, and M. Luo.** 2004. An exposed domain in the severe acute respiratory syndrome coronavirus spike protein induces neutralizing antibodies. J. Virol. **78:**7217–7226.
39. **Zwick, M. B., A. F. Labrijn, M. Wang, C. Spenlehauer, E. Ollmann Saphire, J. M. Binley, J. P. Moore, G. Stiegler, H. Katinger, D. R. Burton, and P. W. H. I. Parren.** 2001. Broadly neutralizing antibodies targeted to the membrane-proximal external region of human immunodeficiency virus type 1 glycoprotein gp41. J. Virol. **75:**10892–10905.
40. **Zwick, M. B., M. Wang, P. Poignard, G. Stiegler, H. Katinger, D. R. Burton, and P. W. Parren.** 2001. Neutralization synergy of human immunodeficiency virus type 1 primary isolates by cocktails of broadly neutralizing antibodies. J. Virol. **75:**12198–12208.
41. **Zwick, M. B., R. Jensen, S. Church, M. Wang, G. Stiegler, R. Kunert, H. Katinger, and D. R. Burton.** 2005. Anti-human immunodeficiency virus type 1 (HIV-1) antibodies 2F5 and 4E10 require surprisingly few crucial residues in the membrane-proximal external region of glycoprotein gp41 to neutralize HIV-1. J. Virol. **79:**1252–1261.